

Electron-plasmon scattering in chiral 1D systems with nonlinear dispersion

M. Heyl,¹ S. Kehrein,¹ F. Marquardt,^{1,2} and C. Neuenhahn^{1,2}

¹*Department of Physics, Arnold Sommerfeld Center for Theoretical Physics, and Center for NanoScience, Ludwig-Maximilians-Universität München, Theresienstr. 37, 80333 Munich, Germany*

²*Institut für Theoretische Physik, Universität Erlangen-Nürnberg, Staudtstr. 7, 91058 Erlangen, Germany*

We investigate systems of spinless one-dimensional chiral fermions realized, e.g., in the arms of electronic Mach-Zehnder interferometers, at high energies. Taking into account the curvature of the fermionic spectrum and a finite interaction range, we find a new scattering mechanism where high-energy electrons scatter off plasmons (density excitations). This leads to an exponential decay of the single-particle Green's function even at zero temperature with an energy-dependent rate. As a consequence of this electron-plasmon scattering channel, we observe the coherent excitation of a plasmon wave in the wake of a high-energy electron resulting in the buildup of a monochromatic sinusoidal density pattern.

PACS numbers: 71.10.Pm, 72.15.Nj, 71.10.-w

Many-particle physics in one dimension drastically differs from that in higher dimensions. In higher dimensions within the scope of Fermi liquid theory, the presence of interactions between fermions does not change the character of the elementary low-energy excitations that are still fermionic. In one dimension this is completely different. Even weak interactions alter the character of the low-energy excitations. They become bosonic and of collective nature. Recently, however, it has been shown that 1D fermionic systems show Fermi liquid-like behavior at higher energies if one accounts for the curvature in the spectrum [1].

In this work we consider the properties of a system of spinless 1D chiral fermions under the injection of a high-energy fermion with well-defined energy ε beyond the low-energy paradigm. We take into account the influence of the curvature of the fermionic dispersion and a finite-range interaction. In experiments, electrons with well defined energy may be injected via a quantum dot filter into an integer quantum hall edge state [2, 3]. Employing these edge channels as the arms of electronic Mach-Zehnder interferometers [4–8], for example, one may investigate the decoherence of the injected electrons as a function of injection energy ε . In this regard, we analyze the Green's function (GF) $G^>(x, \varepsilon) = -i \int dt e^{i\varepsilon t} \langle \hat{\psi}(x, t) \hat{\psi}^\dagger(0, 0) \rangle$ (which, in the context of MZI's, is directly related to the interference contrast [9]), the spectral function $A(k, \varepsilon)$ and the density $\varrho(x, t)$ of the fermionic background in presence of the high-energy fermion.

Our main observation is the existence of a new scattering mechanism in chiral 1D systems at high energies due to an interplay of both curvature and finite interaction range. A fermion injected with a high energy such that it experiences the curvature of the spectrum scatters off low-energy density excitations, so-called plasmons. This gives rise to an exponential decay of the GF in the large distance limit with a nonzero decay rate Γ_ε even at zero temperature in stark contrast to the low-energy

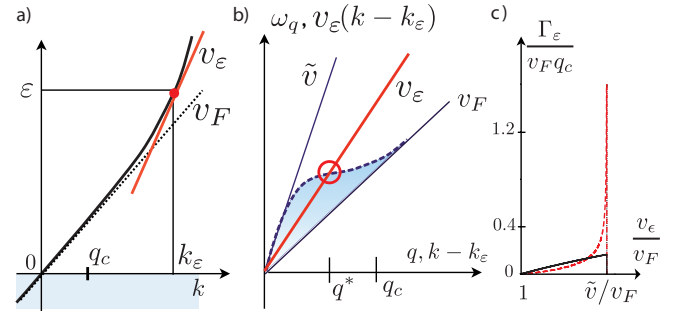


Figure 1: (color online) a) High energy fermion injected with energy $\varepsilon \gg q_c v_F$ on top of the Fermi sea. Due to the curvature of the dispersion it moves with an energy-dependent velocity $v_\varepsilon \geq v_F$ b) Sketch of the dispersion relation of the density excitations of the Luttinger liquid (plasmons) ω_q with the plasmon velocity \tilde{v} (blue line) and the dispersion of the high-energy fermion linearized in the vicinity of its initial energy ε (red line). The mode q^* denotes the intersection point of the two dispersion relations whose existence is responsible for momentum and energy conserving scattering between the injected electron and the plasmons. c) Plot of the decay rate of the GF [cf. Eq. (3)] for an analytic interaction potential $U_q = 2\pi\alpha v_F e^{-(q/q_c)^2}$ (dashed line) and a nonanalytic one $U_q = 2\pi\alpha v_F e^{-|q/q_c|}$ (solid line), respectively (see main text).

case where the asymptotic behavior is algebraic. The excitation of plasmons happens coherently leading to the buildup of a sinusoidal density pattern in the fermionic density in the wake of the injected high-energy electron.

At low energies, interacting 1D fermions are described perfectly well by a linearized spectrum and a subsequent application of the bosonization technique. Taking into account curvature one has to employ new methods. Recently, there has been considerable progress in calculating single-particle properties beyond the low-energy paradigm [1, 10–14]. In Ref. [11] edge singularities in the dynamic structure factor were found by performing a projection scheme in analogy to the X-ray edge singularity problem. The authors of [12, 13] provided a

framework for the calculation of response functions for pointlike interactions beyond the perturbative regime. In a combined Bethe Ansatz and tDMRG analysis it was shown that the edge behavior of the spectral function is indeed described by X-ray edge type effective Hamiltonians and the exact singularity exponents have been determined [14].

For the calculation of the GF and the spectral function we employ two different methods that turn out to yield exactly the same result. On the one hand, we use a physically transparent semiclassical ansatz whose validity was proven earlier by comparison to the bosonization result [9]. This ansatz is naturally extended to include curvature effects. Additionally, we derive an effective Hamiltonian for the description of the single-particle properties by extending the method of Pustilnik *et al.* [11] to include the full interaction potential. Based on the latter approach we also obtain the fermionic density after the injection of the high-energy electron.

Model and GF. Consider a system of spinless chiral interacting 1D electrons described by the Hamiltonian

$$\hat{H} = \sum_k \varepsilon_k : \hat{c}_k^\dagger \hat{c}_k : + \frac{1}{2} \int dx dx' \hat{\rho}(x) U(x-x') \hat{\rho}(x') \quad (1)$$

where $\hat{\psi}(x) = 1/\sqrt{L} \sum_k e^{ikx} \hat{c}_k$ and we normal order the Hamiltonian with respect to the vacuum (indicated by $: \dots :$) where all states with $k < 0$ are occupied and empty otherwise. We denote the fermionic density with $\hat{\rho}(x) = : \hat{\psi}^\dagger(x) \hat{\psi}(x) :$ and introduce an almost arbitrary interaction potential $U(x)$ with a Fourier transform $U_q \equiv \int dx e^{-iqx} U(x)$. The latter is assumed to be cut-off beyond some momentum scale q_c , and we introduce a dimensionless coupling strength $\alpha = U_{q=0}/2\pi v_F$. Whereas the following considerations in principle do not rely on a particular choice of ε_k , for simplicity, we deal with a dispersion relation of positive curvature as in the case of free fermions and assume a repulsive interaction, i.e., $\alpha > 0$.

It will be shown below that due to the finite interaction range the indistinguishability between the injected fermion and the Fermi sea at small temperatures is lifted if the injection energy $\varepsilon \gg v_F q_c$ is sufficiently large. This allows for the separation of the high- and low-energy degrees of freedom, the single fermion propagating ballistically with the bare velocity v_ε and the remaining fermions constituting a Tomonaga-Luttinger liquid, respectively. The bosonic excitations of the latter evolve according to the plasmonic dispersion relation $\omega_q = v_F q(1 + U_q/2\pi v_F)$ defining the velocity $\tilde{v} = v_F(1 + \alpha)$ of the fastest plasmon.

The fermion and the plasmons are coupled via a residual interaction. Due to the finite interaction range $1/q_c$ and as long as $v_F < v_\varepsilon < \tilde{v}$ there exists an intersection point q_* (with $\omega_{q_*} = v_\varepsilon q_*$) between the plasmonic spectrum and the dispersion relation of the single fermion $\varepsilon_k - \varepsilon \approx v_\varepsilon(k - k_\varepsilon)$ linearized in the vicinity of its initial

energy [see Fig. (1)]. The existence of the intersection point enables an electron-plasmon scattering mechanism conserving momentum and energy. This manifests in an exponential long-distance decay of the GF even at zero temperature $T = 0$:

$$|G^>(x, \varepsilon)| \sim x^{-\gamma_\varepsilon} e^{-\Gamma_\varepsilon x/v_\varepsilon}, \quad xq_c \gg 1, \quad (2)$$

with

$$\Gamma_\varepsilon = 2\pi^2 \frac{(v_\varepsilon - v_F)^2}{|U'_{q_*}|} \Theta(\tilde{v} - v_\varepsilon), \quad \gamma_\varepsilon = \left[\frac{\alpha v_F}{\tilde{v} - v_\varepsilon} \right]^2. \quad (3)$$

A plot of the decay rate Γ_ε is shown in Fig. (1). The appearance of the step function Θ in the expression for Γ_ε mirrors the fact that for $v_\varepsilon > \tilde{v}$ the high-energy electron is faster than any plasmonic mode such that the intersection point q_* between the plasmonic and fermionic dispersion relation vanishes [cf. Fig. (1)]. In the limit of vanishing curvature, i.e., $v_\varepsilon \rightarrow v_F$ we have $\Gamma_\varepsilon \rightarrow 0$ and a power-law exponent $\gamma_\varepsilon \rightarrow 1$, which is independent of the coupling strength α as found earlier [9]. Increasing the injection energy such that $v_\varepsilon \rightarrow \tilde{v}$, the decay rate diverges for analytic interaction potentials. In the limit of large energies, where $v_\varepsilon > \tilde{v}$ and $\Gamma_\varepsilon = 0$, the GF decays algebraically for long distances. This decay can be attributed to the Anderson Orthogonality catastrophe [15] in view of the fact that the GF is the equivalent to the core hole Green's function in the X-ray edge singularity problem. In this context it is remarkable that the exponent $\gamma_\varepsilon = \Delta n^2$ can be related to the screening charge Δn , that is the charge displaced in the fermionic background by the injection of the high-energy fermion. In the remainder of this article, we will sketch the derivation of Eq. (2) and discuss further quantities such as the spectral function and the density of the fermionic background after the injection of the high-energy electron.

Semiclassical Ansatz for the GF. Motivated by the earlier results in Ref. [9] we employ a semiclassical ansatz for the GF in the limit of large energies $\varepsilon \gg q_c v_F$. After its injection, the electron propagates chirally with its bare velocity v_ε , thereby experiencing a fluctuating potential landscape $\hat{V}(t) = \int dx' U(x' - v_\varepsilon t) \hat{\rho}_B(x', t)$ [see also [16]] at its classical position $x = v_\varepsilon t$. Here, $\hat{\rho}_B(x, t)$ is the fermionic density $\hat{\rho}_B(x, t) = L^{-1} \sum_{q>0} \sqrt{n_q} (\hat{b}_{q,B} e^{iqx - i\omega_q t} + \text{h.c.})$ [with $(n_q = qL/2\pi)$] of the bath electrons with bosonic operators $\hat{b}_{q,B} = 1/\sqrt{n_q} \sum_k \hat{c}_{k,B}^\dagger \hat{c}_{k+q,B}$ representing the plasmonic excitations evolving according to the plasmonic dispersion ω_q . It is assumed that the non-linearity of the fermionic dispersion is small enough such that the velocity of the propagating fermion can be considered as constant and the remaining electrons can be treated by means of bosonization. Specifically, the change in velocity of an electron

due to a scattering event with a typical momentum transfer q_c has to be small such that $q_c \partial^2 \varepsilon_k / \partial k^2 \ll \partial \varepsilon_k / \partial k$ for all momenta k near the Fermi momentum and near k_ε . As a consequence of the fluctuating plasmonic quantum bath, the high-energy fermion accumulates a random phase and its non-interacting GF is multiplied by the average value of the corresponding phase factor:

$$\frac{G^>(x, \varepsilon)}{G_0^>(x, \varepsilon)} = \left\langle \hat{T} \exp \left[-i \int_0^{x/v_\varepsilon} dt' \hat{V}(t') \right] \right\rangle. \quad (4)$$

Here, \hat{T} denotes the time ordering symbol and $G_0^> = -i e^{i k_\varepsilon x} / v_\varepsilon$ is the non-interacting GF for $\varepsilon > 0$. Note that the whole influence of the finite curvature is contained in the energy dependence of $v_\varepsilon \geq v_F$. Employing the Gaussian nature of the plasmonic bath it is possible to express the r.h.s. of Eq. (4) in terms of the auto-correlation function of the potential fluctuations $\langle \hat{V} \hat{V} \rangle_\omega = \int dt e^{i \omega t} \langle \hat{V}(t) \hat{V}(0) \rangle$ (cf. [9]) experienced by the single electron in its co-moving frame of reference. In particular, for the modulus of the GF one obtains

$$\left| \frac{G^>}{G_0^>} \right| = \exp \left[- \int_{-\infty}^{\infty} \frac{d\omega}{2\pi} \frac{\sin^2(\omega x / 2v_\varepsilon)}{\omega^2} \langle \{ \hat{V}, \hat{V} \} \rangle_\omega \right] \quad (5)$$

where only the symmetrized correlator $\langle \{ \hat{V}, \hat{V} \} \rangle_\omega = \langle \hat{V} \hat{V} \rangle_\omega + \langle \hat{V} \hat{V} \rangle_{-\omega}$ enters. The asymptotic long-distance decay of the GF in Eq. (7) is governed by the low-frequency properties of the potential fluctuation spectrum $\langle \{ \hat{V}, \hat{V} \} \rangle_{\omega \downarrow 0} = 2\pi \gamma_\varepsilon |\omega| + 4\Gamma_\varepsilon$ (here we took $T = 0$). It consists of an Ohmic part responsible for the power-law decay and a constant offset which leads to an exponential decay of the GF. For intermediate energies where $v_F q_c \ll \varepsilon$ but $v_\varepsilon = v_F$, Eq. (4) reproduces exactly the GF from standard bosonization [9]. Thus, our analysis is correct within the validity of the bosonization technique.

Effective Hamiltonian. In fact, the semiclassical ansatz for the GF in Eq. (4) matches precisely the result obtained by an extension of the approach in Ref. [11] to treat the full interaction potential. There, $G^>(x, t)$ is viewed as an impurity problem related to the X-ray edge singularity [17] where a scatterer, the injected fermion in this case, is suddenly switched on. The Hamiltonian in Eq. (1) is projected onto two strips of states that capture the relevant degrees of freedom, an energy interval around the initial energy ε of the injected high-energy fermion labeled by ε and an energy window around the Fermi energy labeled by an index B . Under this projection, the fermionic field decomposes into $\hat{\psi}(x) \rightarrow \hat{\psi}_B(x) + e^{i k_\varepsilon x} \hat{\psi}_\varepsilon(x)$. Linearizing the dispersion relations within both strips of states, the Hamiltonian of the low-energy sector can be bosonized. Regarding correlation functions involving at most one high-energy electron one obtains:

$$H = \sum_{q>0} \omega_q b_{q,B}^\dagger b_{q,B} + \int dx \hat{\psi}_\varepsilon^\dagger(x) (\varepsilon - i v_\varepsilon \partial_x) \hat{\psi}_\varepsilon(x)$$

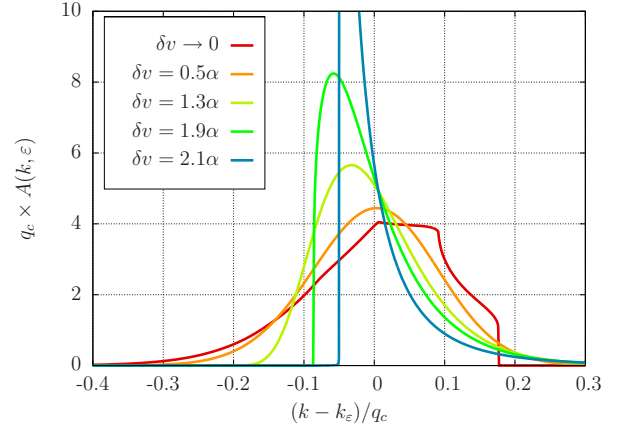


Figure 2: (color online) Spectral function $A(k, \varepsilon)$ for different velocities v_ε of the high-energy fermion where $\delta v = (v_\varepsilon - v_F)/v_F$. For these plots we have chosen an analytic potential $U_q = 2\pi v_F \alpha \exp[-(q/q_c)^2]$ with $\alpha = 0.2$.

$$+ \int dx dx' \hat{\rho}_B(x) U(x - x') \hat{\psi}_\varepsilon^\dagger(x') \hat{\psi}_\varepsilon(x'). \quad (6)$$

In the derivation of this effective Hamiltonian a contribution proportional to U_{k_ε} has been neglected as $k_\varepsilon \gg q_c$ and U_q rapidly decays for $q \gg q_c$ by assumption. The omitted term is responsible for exchange processes between the high- and low-energy sector lifting the distinguishability between the high-energy fermion and the low-energy degrees of freedom. In Eq. (6) a constant Fock shift $U(x=0) \hat{N}_\varepsilon / 2$ is omitted which drops out automatically if we take as a starting point the Coulomb interaction instead of the density-density interaction in Eq. (1). The Hamiltonian in Eq. (6) can be diagonalized by means of the unitary transformation $\hat{U} = \exp(\hat{S})$ where $\hat{S} = \int dx \hat{\psi}_\varepsilon(x) \hat{\psi}_\varepsilon(x) \sum_{q>0} \chi_q [\hat{b}_{q,B}^\dagger e^{-iqx} - H.c.]$ with $\chi_q = 2\pi U_q / (U_q - 2\pi(v_\varepsilon - v_F)) \sqrt{n_q}$. From Eq. (6), one can calculate the golden rule rate for the excitation of plasmons by the high-energy fermion. It matches precisely the decay rate determining the exponential decay of the GF in Eq. (3).

Spectral function. The spectral function $A(k, \varepsilon)$ is connected to the GF via $A(k, \varepsilon) = i/(2\pi) \int dx e^{-ikx} G^>(x, \varepsilon)$ ($\varepsilon > 0$ and $T = 0$). It behaves qualitatively different whether the exponent γ_ε appearing in the large distance behavior of the GF is bigger or smaller than one. Remarkably, this property is not connected to the distinction between $v_\varepsilon \leq \tilde{v}$ that determines the threshold between exponential and algebraic large distance behavior for the GF. For $\gamma_\varepsilon < 1$ or equivalently $\delta v = (v_\varepsilon - v_F)/v_F > 2\alpha$, the spectral function shows a power-law singularity together with a threshold behavior for $k \rightarrow \kappa_\varepsilon + k_\varepsilon$

$$A(k, \varepsilon) \sim \sin(\gamma_\varepsilon \pi / 2) (k - \kappa_\varepsilon - k_\varepsilon)^{\gamma_\varepsilon - 1} \theta(k - \kappa_\varepsilon - k_\varepsilon)$$

where $\kappa_\varepsilon = v_\varepsilon^{-1} \mu_\varepsilon$ and $\mu_\varepsilon = \int_0^\infty dq (U_q / 2\pi)^2 / (v_\varepsilon - v_F - U_q / 2\pi)$ denotes the energy that is needed to overcome

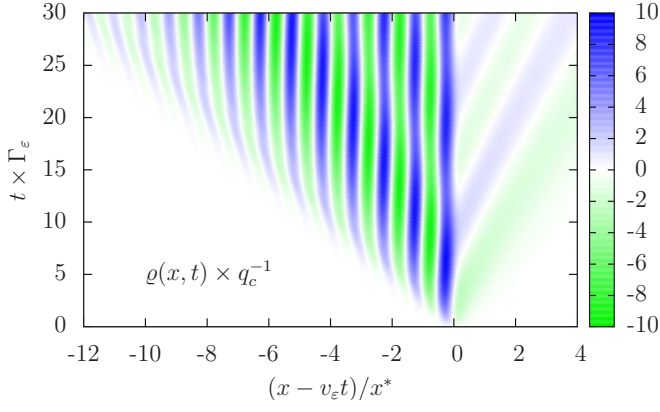


Figure 3: (color online) The fermionic density $\rho(x, t)$ in the co-moving frame of the high-energy electron injected at time $t = 0$. The period x^* of the oscillations is given by $x^* = 2\pi/q_*$. For this plot we have chosen the same potential U_q as in Fig. 2 and $\delta v = 0.5\alpha$.

the Coulomb interaction while injecting an electron with energy ε . In Fig. (2), the curve with $\delta v = 2.1\alpha$ shows the spectral function with a power law singularity according to Eq. (7). Note that the support of the spectral function, $A(k, \varepsilon) \neq 0$ only for $\varepsilon + \mu_\varepsilon < \varepsilon_k$, is exactly opposite to the low-energy Tomonaga-Luttinger Liquid case where $A(\varepsilon, k) \neq 0$ only for $\varepsilon + \mu_\varepsilon > \varepsilon_k$. This is a consequence of the condition $v_\varepsilon > \tilde{v}$ implying that an electron with wave vector k can excite plasmonic modes only by reducing the energy in the system [see Fig. 1]. In the limit $\varepsilon \rightarrow \infty$ where $\gamma_\varepsilon \rightarrow 0$, one recovers the free particle, a δ -function in the spectrum as $\lim_{\eta \rightarrow 0} \eta |x|^{7-1}/2 = \delta(x)$. As shown in Ref. [18] this is not the case for a linearized dispersion even in the limit $\varepsilon \rightarrow \infty$.

For $\gamma_\varepsilon > 1$, i.e. $v_F < v_\varepsilon < 2\tilde{v} - v_F$, the spectrum changes drastically. The singularity vanishes and the spectral function merely becomes a skew Gaussian, compare Fig. (2). In the regime $\gamma_\varepsilon > 1$ the GF, that is the Fourier transform of $A(k, \varepsilon)$, is dominated by its initial Gaussian decay due to strong dephasing by the plasmonic background fluctuations. Thus, the spectrum itself is also dominated by the incoherent background such that no well-defined quasiparticle peak is visible in spite of the exponential decay of the GF. In the limit $v_\varepsilon \rightarrow v_F$ and for a potential U_q with a sharp cutoff at q_c , one recovers the result by Ref. [18] as indicated in Fig. (2).

Coherent emission of plasmon waves. In order to investigate the influence of the electron-plasmon scattering mechanism onto the fermionic background, we analyze the fermionic density of the bath

$$\rho(x, t) = \mathcal{N} \langle \psi_0 | \hat{\psi}_\varepsilon(0) \hat{\rho}_B(x, t) \hat{\psi}_\varepsilon^\dagger(0) | \psi_0 \rangle \quad (8)$$

in the presence of the high-energy electron. Here, $|\psi_0\rangle$ is the ground state of the Hamiltonian in Eq. (6) without the high-energy fermion and $\mathcal{N} = \langle \psi_0 | \hat{\psi}_\varepsilon(0) \hat{\psi}_\varepsilon^\dagger(0) | \psi_0 \rangle^{-1}$ a normalization constant. In the parameter regime $v_\varepsilon <$

\tilde{v} where electron-plasmon scattering takes place one observes the coherent emission of plasmon waves with wave vector q_* of the resonant plasmonic mode [see Fig. (3)]. In the limit $t \rightarrow \infty$ and for distances $x - v_\varepsilon t \gg q_c^{-1}$ sufficiently far away from the position of the high-energy electron, we obtain the following analytic result:

$$\rho(x, t) \rightarrow \Theta(v_\varepsilon t - x) \sin[q_*(x - v_\varepsilon t)] U_{q_*}/U'_{q_*} \quad (9)$$

As can be seen in Fig. (3), the coherent density excitations build up within a 'light cone' $x \in [v_F t, \tilde{v} t]$ [19] set by the minimal and maximal plasmonic phase velocities. The wavelength of the oscillations in the density $\rho(x, t)$ is tunable by the choice of an appropriate injection energy ε of the high-energy fermion.

For velocities $v_\varepsilon > \tilde{v}$, no scattering between electrons and plasmons is possible. In this case, the density $\rho(x, t)$ can be separated into two contributions. The first one describes the initial excitation of plasmonic modes right after the injection of the high-energy fermion. This transient perturbation cannot follow the electron that is faster than any plasmonic mode. The second contribution traveling together with the high-energy electron is responsible for the screening of the injected charge and is reminiscent of viewing the GF as an impurity problem. Integrating over space then provides us with the screening charge Δn , the charge displaced by the introduction of the local scatterer. As mentioned before, it is directly related to the exponent $\gamma_\varepsilon = \Delta n^2$ of the GF.

Conclusions. We have discussed electron-plasmon scattering in systems of 1D chiral electrons. This scattering leads to an exponential decay of the single-particle Green's function even at zero temperature and to a coherent monochromatic pattern in the fermionic density in the wake of the electron. This effect is absent in the low-energy limit and relies exclusively on the interplay between a finite interaction range and a non-linear fermionic dispersion.

Acknowledgements. We thank L. Glazman for fruitful discussions. Financial support by NIM, CeNS, the Emmy-Noether program and the SFB/TR 12 is gratefully acknowledged.

-
- [1] M. Khodas, M. Pustilnik, A. Kamenev, and L. I. Glazman, Phys. Rev. B **76**, 155402 (2007).
 - [2] G. Feve, A. Mahe, J.-M. Berroir, T. Kontos, B. Placais, D. C. Glatli, A. Cavanna, B. Etienne, and Y. Jin, Science **316**, 1169 (2007).
 - [3] C. Altimiras, H. le Sueur, U. Gennser, A. Cavanna, A. Mailly, and F. Pierre, Nature Phys. **6**, 34 (2009).
 - [4] Y. Ji, Y. Chung, D. Sprinzak, M. Heiblum, D. Mahalu, and H. Shtrikman, Nature **422**, 415 (2003).
 - [5] I. Neder, M. Heiblum, Y. Levinson, D. Mahalu, and V. Umansky, Phys. Rev. Lett. **96**, 016804 (2006).

- [6] L. V. Litvin, H.-P. Tranitz, W. Wegscheider, and C. Strunk, Phys. Rev. B **75**, 033315 (2007).
- [7] P. Roulleau, F. Portier, D. C. Glatthli, P. Roche, A. Cavanna, G. Faini, U. Gennser, and D. Mailly, Phys. Rev. B **76**, 161309(R) (2007).
- [8] L. V. Litvin, A. Helzel, H.-P. Tranitz, W. Wegscheider, and C. Strunk, Phys. Rev. B **78**, 075303 (2008).
- [9] C. Neuenhahn and F. Marquardt, Phys. Rev. Lett. **102**, 046806 (2009).
- [10] A. V. Rozhkov, Eur. Phys. J. B **47**, 193 (2005).
- [11] M. Pustilnik, M. Khodas, A. Kamenev, and L. I. Glazman, Phys. Rev. Lett. **96**, 196405 (2006).
- [12] A. Imambekov and L. I. Glazman, Science **323**, 228 (2009).
- [13] A. Imambekov and L. I. Glazman, Phys. Rev. Lett. **102**, 126405 (2009).
- [14] R. G. Pereira, S. R. White, and I. Affleck, Phys. Rev. B **79**, 165113 (2009).
- [15] P. W. Anderson, Phys. Rev. Lett. **18**, 1049 (1967).
- [16] K. Le Hur, Phys. Rev. Lett. **95**, 076801 (2005).
- [17] P. Nozieres and C. T. De Dominicis, Phys. Rev. **178**, 1097 (1969).
- [18] K. Schönhammer and V. Meden, Phys. Rev. B **47**, 16205 (1993).
- [19] P. Calabrese and J. Cardy, Phys. Rev. Lett. **96**, 136801 (2006).